Available online at www.sciencedirect.com
ScienceDirect
Ceramics International 33 (2007) 1481–1487
CERAMICS INTERNATIONAL
www.elsevier.com/locate/ceramint

# Synthesis and characterization of $MgSiO_3$-containing glass-ceramics

A. Goel [a], D.U. Tulyaganov [b], S. Agathopoulos [c], M.J. Ribeiro [d], J.M.F. Ferreira [a,*]

[a] Department of Ceramics and Glass Engineering, University of Aveiro, CICECO, 3810-193 Aveiro, Portugal
[b] Scientific Research Institute of Space Engineering, 700128 Tashkent, Uzbekistan
[c] Department of Materials Science and Engineering, University of Ioannina, GR-451 10 Ioannina, Greece
[d] UIDM, ESTG, Polytechnique Institute of Viana do Castelo, 4900 Viana do Castelo, Portugal

Received 22 March 2006; received in revised form 1 May 2006; accepted 25 May 2006
Available online 11 September 2006

**Abstract**

Three glass compositions, aiming at producing Mg-metasilicate ($MgSiO_3$) based glass-ceramics, were investigated. The composition with 25 mol% diopside and 75 mol% enstatite ($Ca_{0.125}Mg_{0.875}SiO_3$), considered as the starting point, aimed to reduce the tendency of Mg-metasilicate for polymorphism. In the two derivative compositions, substitutions of yttrium and barium for magnesium as well as boron for silicon were attempted. Glasses in both bulk and frit forms were produced by melting in alumina crucibles at 1600 °C for 1–2 h. Sintering and crystallization of glass-powder compacts were carried out at different temperatures in the range of 850–1000 °C. The influence of these substitutions on the crystallization process of the glasses and the properties of the resultant glass-ceramics was experimentally determined and discussed in the light of the potential of these compositions in applications of advanced technology.


*Keywords:* B. Microstructure-final; D. Glass-ceramics; E. Functional applications; Mg-metasilicate

## 1. Introduction

Ceramic and glass-ceramic (GC) materials based on magnesium metasilicates ($MgSiO_3$) are ideal for high frequency low loss high voltage insulators, surge arrestors, standoffs, spacers, resistor and coil forms due to their good mechanical and low loss electrical properties [1–4]. Enstatite is a low temperature modification of $MgSiO_3$, which, during a thermal circle, transforms into proto-enstatite (during heating) and clino-enstatite (during cooling of proto-enstatite) [1–3,5]. The presence of metastable proto-enstatite can result in electrical loss and weakening of mechanical strength during operation conditions. This drawback is known from the technology of steatite ceramics [2,5,6]. Another striking disadvantage of steatite ceramics is the narrow sintering range due to the rapid formation of liquid phase during firing [5].

Several attempts have been addressed in producing $MgSiO_3$ based materials using GC route. It must be noted that the precise stoichiometric composition of enstatite does not result in a stable glass. Lee and Heuer have presented an attempt to produce stoichiometric $MgSiO_3$ glass by quenching of glass melt into water where liquid $N_2$ was bubbling [2]. In 1974, Takher et al. [7–9] developed steatite-based GCs with a wide sintering range using glass powder of $MgO–BaO–Al_2O_3–SiO_2$ system [7,8]. The glass was melted in quartz crucibles at 1520 °C. Using glass powders with surface area of 0.5–0.7 $m^2/g$, the sintering range was widened up to 80° (between 1080 °C and 1160 °C), while the optimum firing temperature was 1120 °C. The dielectric performance of the sintered steatite GCs was improved by adding BaO and ZnO in the initial glass batch [7,9]. That particular composition exhibited reduced dielectric loss angle (tan $\delta$ at 1 MHz decreased down to 0.0008–0.0009) [9].

In 1991, Beall [10] successfully developed enstatite GCs in the ternary $MgO–Al_2O_3–SiO_2$ system using tetragonal zirconia as nucleation agent. In the base glass, tetragonal zirconia was formed as a primary crystal phase at 800–900 °C. Proto-enstatite was subsequently formed after heat treatment above 900 °C and transformed into fine crystals of twinned clino-enstatite (but not orthoenstatite) during cooling. The resultant GCs had fracture toughness of ca. 5 MPa $m^{0.5}$. Compositions with high content of zirconia also exhibited excellent refractoriness. Beyond bulk nucleation processing, Echeverria and Beall [11] have also produced enstatite GCs via surface nucleation mechanism and sol–gel route, achieving toughness of ca. 4 MPa $m^{0.5}$.

* Corresponding author. Tel.: +351 234 370242; fax: +351 234 425300.
*E-mail address:* jmf@cv.ua.pt (J.M.F. Ferreira).

0272-8842/$32.00 
doi:10.1016/j.ceramint.2006.05.012

Table 1
Compositions of the parent glasses

| Glass | | MgO | CaO | BaO | $SiO_2$ | $B_2O_3$ | $Al_2O_3$ | $Y_2O_3$ |
|---|---|---|---|---|---|---|---|---|
| 1, $Ca_{0.125}Mg_{0.875}SiO_3$ | wt.% | 34.45 | 6.85 | – | 58.70 | – | – | – |
| | mol% | 43.75 | 6.25 | – | 50.00 | – | – | – |
| | mol ratio | 7 | 1 | – | 8 | – | – | – |
| 2, $Y_{0.125}Mg_{0.875}Si_{0.875}B_{0.125}O_3$ | wt.% | 33.17 | – | – | 49.45 | 4.09 | – | 13.27 |
| | mol% | 46.67 | – | – | 46.67 | 3.33 | – | 3.33 |
| | mol ratio | 14 | – | – | 14 | 1 | – | 1 |
| 3, $Y_{0.125}Mg_{0.725}Ba_{0.15}Si_{0.875}B_{0.125}O_3$ | wt.% | 23.70 | – | 18.65 | 42.65 | 3.52 | – | 11.44 |
| | mol% | 38.67 | – | 8.00 | 46.67 | 3.33 | – | 3.33 |
| | mol ratio | 11.61 | – | 2.40 | 14 | 1 | – | 1 |

*Note*: 1.00 wt.% NiO was added in the batches.

Different types of enstatite GC materials have been produced by Partridge et al. and Budd [1,12–14] for application in electronic circuits. When both $ZrO_2$ and $TiO_2$ were used as nucleating agents, the sintered GCs had flexural strength of 250 MPa, fracture toughness of 3.3 MPa $m^{0.5}$, and fracture surface energy of 51 J/$m^2$.

In the crystalline lattice of Mg-metasilicate there are two non-equivalent chains, where one half of Mg cations occupy symmetrical (or regular) octahedral positions, while the second half occupy irregular octahedral positions [15–18]. This feature allows half of $Mg^{2+}$ to be replaced by $Ca^{2+}$, despite the significant difference of their ion size (40%). Such a substitution can result in formation of a more stable diopside structure. Intermediate compositions of synthetic clino-pyroxens in the diopside-enstatite joint form continuous solid solutions with a general formula of $Ca_xMg_{1-x}SiO_3$ (Di-En). According to Vereshchagin et al. [18], compositions with less than 12 mol% of diopside in the Di-En joint are prone to polymorphism.

In the present study, partial substitutions in cation and anion sublattice of Mg-metasilicate were attempted and their influence on crystallization process and the properties of the resultant GCs was investigated. Three glass compositions, presented in Table 1, were investigated. The designations 1, 2, and 3 correspond both to the glasses and the GCs. The composition with 25 mol% diopside and 75 mol% enstatite ($Ca_{0.125}Mg_{0.875}SiO_3$, composition 1) was considered as the starting point, aiming at reducing the tendency of Mg-metasilicate for polymorphism. Substitutions of Y for Mg and B for Si were attempted in the composition 2. Composition 3 features a more complex substitution of Y + Ba for Mg and B for Si. The incorporation of $B_2O_3$ in compositions 2 and 3 had a dual aim: to satisfy the overall charge balance of the system, and, under the perspective of technology, to decrease the viscosity of glass melts and facilitate diffusion. To enhance the potential application of the resultant GCs, we incorporated in the batches small amount of NiO (1 wt.%), considering that NiO will favour the adhesion of the resultant GCs with metals.

## 2. Materials and experimental procedure

Powders of technical grade silicon oxide (purity > 99.5%) and calcium carbonate (>99.5%), and of reactive grade $H_3BO_3$, MgO, $Y_2O_3$, $BaCO_3$, and NiO were used. Homogeneous mixtures of batches (~100 g), obtained by ball milling, were preheated at 900 °C for 1 h for decarbonisation and then melted in alumina crucibles at 1600 °C for 1–2 h, in air.

Glasses in bulk form were produced by casting of the melts onto preheated bronze moulds and subsequent immediate annealing at 550 °C (i.e., close to the transformation temperature $T_g$) for 1 h. Glasses in frit form were also obtained by quenching of the melts in cold water. The frit was dried and then milled in a high-speed porcelain mill to obtain fine powders. The powders were granulated (by stirring in a mortar) in a 5 vol.% polyvinyl alcohol solution (PVA, Merck; the solution of PVA was made by dissolution in warm water) in a proportion of 97.5 wt.% of frit and 2.5 wt.% of PVA solution. Rectangular bars with dimensions of 4 mm × 5 mm × 50 mm were prepared by uniaxial pressing (80 MPa). The bars were sintered at four different temperatures (i.e., 850 °C, 900 °C, 950 °C, and 1000 °C). The soaking time at the sintering temperatures was 1 h, while a slow heating rate of 1 K/min aimed to prevent deformation of the samples.

In this study, the following techniques and apparatuses were employed. The particle size distribution of the powders of the frits was determined by light scattering technique (Coulter LS 230, UK, Fraunhofer optical model). The fine milled glass powders were subjected to differential thermal analysis in air (Netzsch 402 EP, Germany; heating rate 5 K/min). Dilatometry measurements were done with annealed bulk glass blocks and sintered rectangular blocks of GCs (Bahr Thermo Analyse DIL 801 L, Germany; heating rate 5 K/min; cross-section of samples 4 mm × 5 mm). The crystalline phases of GC samples in bulk (not powder) form were identified by X-ray diffraction analysis (XRD, Rigaku Geigerflex D/Mac, C Series, Cu Kα radiation, Japan). Copper Kα radiation (λ = 1.5406 nm) produced at 30 kV and 25 mA scanned the range of diffraction angles (2θ) between 10° and 80° with a 2θ-step of 0.02° $s^{-1}$. The phases were identified by comparing the experimental X-ray patterns to standards complied by the International Centre for Diffraction Data (ICDD). Microstructure observations were done at polished (mirror finishing) and then etched (by immersion in 2 vol.% HF solution for 20 s) surfaces of samples by field emission scanning electron microscopy (FE-SEM Hitachi S-4100, Japan; 25 kV acceleration voltage, beam current 10 μA) under secondary electron mode. Energy dispersive spectroscopy (EDS) was employed for chemical

analysis. Archimedes' method (i.e., immersion in diethyl-phthalate) was employed to measure the apparent density of the samples (the mean values and the standard deviations presented have been obtained from 10 different samples). The mechanical properties were evaluated by measurements of three-point bending strength of rectified parallelepiped bars (3 mm × 4 mm × 50 mm) of sintered GCs (Shimadzu Autograph AG 25 TA, 0.5 mm/min displacement; the mean values and their standard deviation presented have been obtained from measurements from 12 bars). The linear shrinkage during sintering was calculated from the difference of the dimensions between the green and the resulting sintered samples (the mean values and the standard deviations presented have been obtained from 10 different samples).

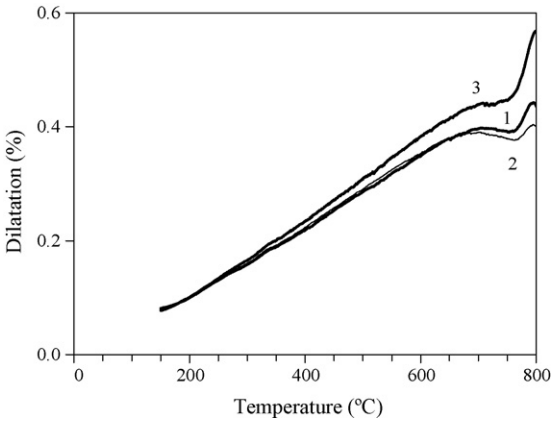


Fig. 2. Dilatometry curves obtained from as-cast and annealed bulk glasses.

## 3. Results and discussion

### 3.1. Casting ability of glasses

The compositions 2 and 3 were prone for easy casting after only 1 h of melting (at 1600 °C), resulting in a homogenous transparent glass with dark honey colour and with no crystalline inclusions, as was also confirmed by X-ray and SEM analyses afterwards. We met, however, some difficulties to produce a stable glass of composition 1, because dwell of 1 h at 1600 °C resulted in a non-homogeneously coloured opaque glass. In particular, the core of the cast bulk glass had a similar aspect to the glasses 2 and 3 but the thick skin layer was opaque brown. SEM observation revealed that the skin layer contained large number of round shaped (300–400 nm) inclusions (Fig. 1) of amorphous nature (confirmed by XRD analysis), which tended to disappear gradually when moving from the skin toward the core of the samples. Prolongation of dwell time to 1.5–2 h eliminated the problem and homogenous transparent glass 1 was obtained.

### 3.2. Thermal analysis of glasses

The curves of thermal expansion of the cast and annealed bulk glasses are plotted in Fig. 2. The transition points ($T_g$) of the investigated glasses ranged between 620 °C and 650 °C, while their softening point ($T_s$) was between 680 °C and 700 °C. From the slope of the linear part of these plots (i.e., 200–500 °C), the thermal expansion coefficients (CTE) of the glasses 1, 2, and 3 were calculated as $6.19 \times 10^{-6}\,K^{-1}$, $6.30 \times 10^{-6}\,K^{-1}$, and $6.88 \times 10^{-6}\,K^{-1}$, respectively. Consequently, the incorporation of $Y_2O_3$, BaO, and $B_2O_3$ in the proportions of investigated compositions (Table 1) favours the increase of CTE of glasses.

The results of the differential thermal analysis (DTA) of the fine powders (obtained from the glass frit), which had mean particle sizes of 3.99 μm, 2.74 μm, and 3.20 μm for the glasses 1, 2, and 3, respectively, and particle size distributions as plotted in Fig. 3, are shown in Fig. 4. A strong exothermic peak, attributed to crystallization, was registered, which was slightly shifted to higher temperatures from glass 1 to glass 3. Shallow exothermic peaks preceded the main crystallization peak at 880–890 °C.

Accordingly, the crystallization temperatures of the glass-powders compacts (i.e., 850–1000 °C) were chosen considering the temperatures of glass transition ($T_g$), the softening point ($T_s$), and the main exothermic peak of crystallization (917–943 °C) [19].

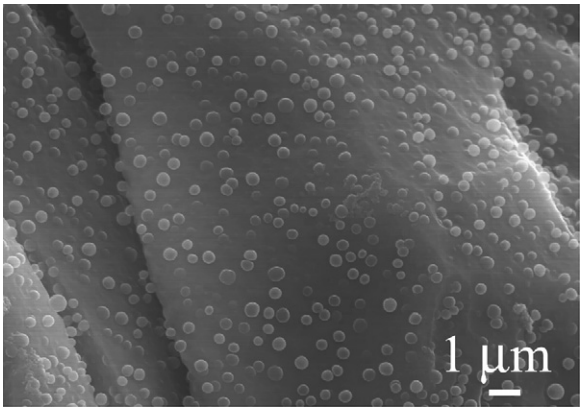


Fig. 1. Inclusions observed at the opaque skin layer of as-cast bulk glass 1 obtained after melting at 1600 °C for 1 h and subsequent annealing.

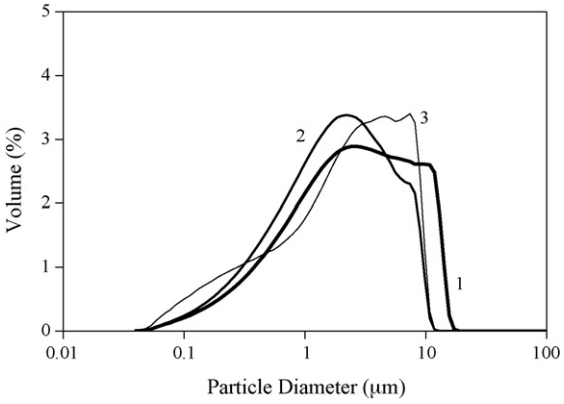


Fig. 3. Particle size distributions of milled glass powders used to prepare the glass-powder compacts.

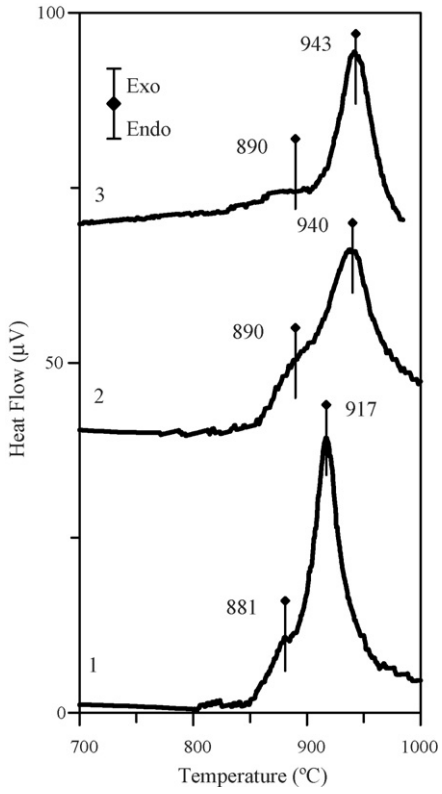


Fig. 4. Differential thermal analysis (DTA) of the investigated glasses from milled fine powders of glass-frits.

### 3.3. Evolution of crystalline phases over increasing temperature

Completely dense samples of dark grey colour but mostly of amorphous nature were obtained after heat treatment at 850 °C of all the glasses, indicating that sintering precedes crystallization. The X-ray diffractograms of glass-powder compacts of composition 1 fired at 850 °C (Fig. 5a) exhibited typical amorphous halo. Quite low intensity peaks of clino-enstatite were also recorded (ICDD card 00-035-0610). Quartz (01-075-1555) is evidently precipitated first in glass 2 after heat treatment at 850 °C (Fig. 5b). Devitrification seemingly occurred more intensively at 850 °C in glass 3 (Fig. 5c), resulting in clear peaks of hexacelsian $BaAl_2Si_2O_8$ (01-088-1051) together with evidence of clino-enstatite (01-075-1404). The presence of the former phase is actually unexpected since no $Al_2O_3$ was incorporated in the batch (Table 1). Evidently, chemical interactions between alumina, due to uptake from the crucible, and the melt took place. EDS analysis of the annealed bulk glasses confirmed presence of $Al_2O_3$ in the amount of 6–7 wt.%.

Increasing intensity of clino-enstatite peaks and appearance of peaks of proto-enstatite (00-011-0273) were observed after heat treatment of compositions 1 and 2 at 900 °C (Fig. 5a and b). The same assemblage of phases was registered in the diffractograms of these glasses after heat treatment at 950 °C and 1000 °C, which suggests a relative stability of phase composition over increasing temperature. However, the diffractogram of composition 2 after heat treatment at 1000 °C suggests the occurrence of some rearrangement of the existing

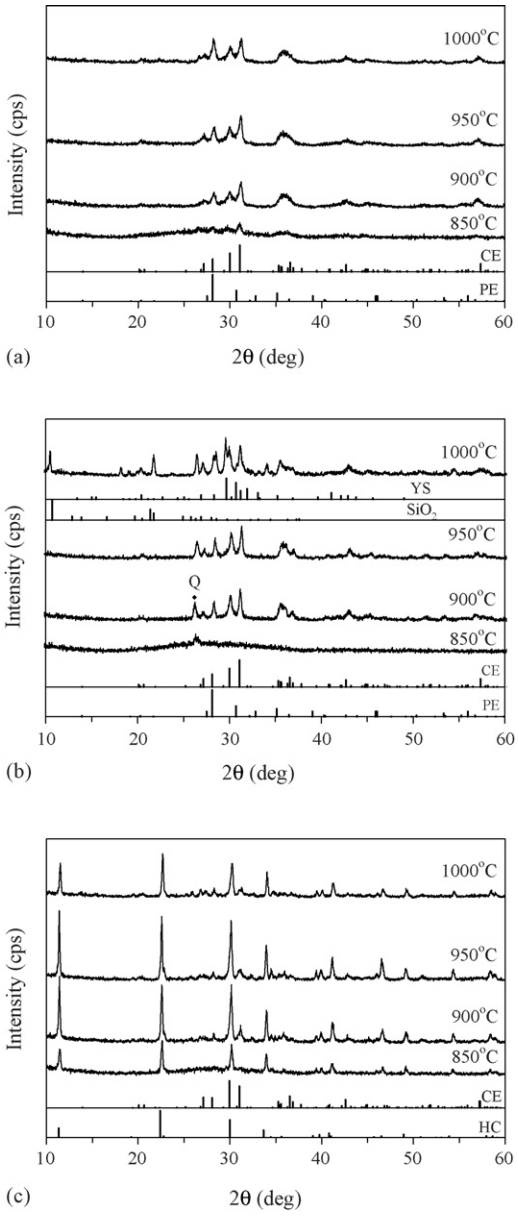


Fig. 5. X-ray diffracrograms of glass-powder compacts after heat treatment at different temperatures of the composition: (a) 1, (b) 2, and (c) 3 (CE: clino-enstatite ICDD card 00-035-0610 for (a and b), and 01-075-1404 for (c); PE proto-enstatite 00-011-0273; $SiO_2$ 00-043-0745; Q: Quartz 01-075-1555; YS: yttrium silicate 00-038-0223; HC: hexacelsian 01-088-1051. The spectra have not been normalized; full scale 5000 cps).

phases, whereby silicon oxide (00-043-0745) (probably a quartz modification) and yttrium silicate (00-038-0223) were identified (Fig. 5b). Consequently, the substitution of Y for Mg in the structure of Mg-metasilicate should take place. The preferable formation of Mg-metasilicate phases (clino- and proto-enstatite) in composition 2 in the temperature range of 900–950 °C supports fairly well this argument.

It is also worthy noting that despite the significant $Al_2O_3$ uptake from the crucibles, no alumina associated phases were identified in the compositions 1 and 2 in the investigated temperature range (Fig. 5a and b). This may suggest that Al cations are mostly accommodated in the Mg-metasilicate structure.

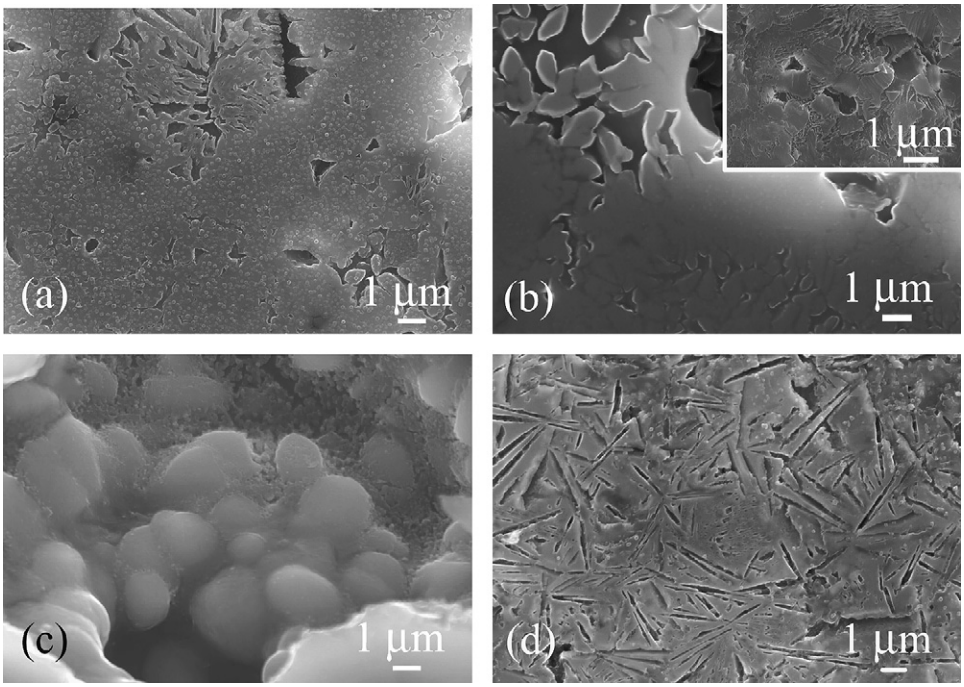


Fig. 6. Microstructure of glass-ceramics (GCs) fired at different temperatures: (a) GC 1, 900 °C; (b) GC 1, 950 °C; (c) GC 2, 950 °C; (d) GC 3, 950 °C (etching with 2 vol.% HF).

The composition 3 exhibited remarkable stability of the phases formed between 850 °C and 1000 °C. The intensity of the peaks of clino-enstatite and hexacelsian increased from 850 °C to 950 °C but further increase of temperature to 1000 °C caused a decay of peaks intensity (Fig. 5c). It is generally known that the crystallization of barium aluminosilicate glasses is faster than in the corresponding calcium or magnesium aluminosilicate glasses [20] due to the lower activation energy of crystallization with barium. In an earlier study [20], formation of celsian with only 3% BaO in the batch was achieved, indicating a strong tendency for celsian formation. A comparative study among aluminosilicates doped with alkaline earth oxides have been carried out in our earlier studies [21,22].

Although thorough investigation of the structures of the polymorphs of $MgSiO_3$ is currently underway, their relative stability is not well understood, yet [2,3,6]. In this work, clino-enstatite was the predominant crystalline phase in the compositions 2 and 3. Proto-enstatite appeared after heat treatment at 900 °C. Lee and Heuer [2] have investigated the crystallization of stoichiometric $MgSiO_3$ glass. They have recorded enstatite and clino-enstatite in the temperature range of 800–1000 °C (dwell 50 h). Proto-enstatite with clino-enstatite kept stable after firing at 1200 °C (dwell 4 h). There are many factors which can affect the proto to clino and the ortho to clino transformations [2,3,6]. Even a simple crushing of the samples can induce such a phenomenon [2]. Therefore, in situ high temperature X-ray analysis will shed light to the relationships of phases in the investigated compositions.

### 3.4. Microstructure of GCs

Typical microstructures of the investigated GCs, produced after firing of glass-powder compacts, are shown in Fig. 6.

Table 2
Properties of the glass-ceramics produced after firing at different temperatures

| Property | Composition | 850 °C | 900 °C | 950 °C | 1000 °C |
|---|---|---|---|---|---|
| Shrinkage (%) | 1 | 14.26 ± 0.38 | 12.98 ± 0.32 | 14.63 ± 0.16 | 13.78 ± 0.26 |
| | 2 | 16.08 ± 0.24 | 16.71 ± 0.65 | 16.53 ± 0.34 | 15.82 ± 0.14 |
| | 3 | 13.01 ± 0.75 | 13.54 ± 0.29 | 13.52 ± 0.32 | 13.81 ± 0.16 |
| Density (g/cm$^3$) | 1 | 2.64 ± 0.02 | 2.60 ± 0.03 | 2.69 ± 0.02 | 2.64 ± 0.03 |
| | 2 | 2.88 ± 0.01 | 2.99 ± 0.005 | 2.99 ± 0.006 | 2.94 ± 0.004 |
| | 3 | 3.14 ± 0.005 | 3.15 ± 0.003 | 3.15 ± 0.006 | 3.10 ± 0.004 |
| Bending strength (MPa) | 1 | 69.67 ± 15.81 | 120.68 ± 10.66 | 109.21 ± 17.23 | 123.97 ± 6.75 |
| | 2 | 84.60 ± 7.26 | 146.59 ± 19.71 | 145.72 ± 17.88 | 113.02 ± 27.59 |
| | 3 | 88.56 ± 9.53 | 115.21 ± 20.55 | 113.78 ± 12.82 | 128.90 ± 16.25 |
| CTE 100–600 °C ($10^{-6}$ K$^{-1}$) | 1 | – | 8.80 | 8.37 | – |
| | 2 | – | 7.77 | 8.41 | – |
| | 3 | – | 8.35 | 9.29 | – |

The observed microstructures agree fairly well with the above results of the X-ray analysis (Fig. 5). In particular, evidence of crystallization was always observed after firing at 900 °C. For the GCs 1 (Fig. 6a), numerous droplets, probably due to phase separation, together with prismatic crystals and some bigger configurations of plate form were observed, all being embedded in a large amount of glassy phase. These crystalline configurations became more evident after firing at 950 °C (Fig. 6b). Fine crystals in the form of twinned clino-enstatite can be easily distinguished.

In the case of composition 2, the evidence of devitrification was clearly observed in the samples fired at 950 °C (Fig. 6c). The complex structure comprised relatively big oval shaped configurations of apparently glassy aspect together with well formed tiny submicron crystals. Several etching schedules were attempted but there was no success to reveal better the structure of the crystals than in Fig. 6c.

The microstructure of GCs 3 was completely different. Crystallization evidently started at lower temperatures (i.e., 850 °C and 900 °C; not shown), as indicated by the X-ray analysis (Fig. 5c), coexisting with a glassy phase. The crystalline features became clearer after heat treatment at 950 °C (Fig. 6d), revealing a dense sintered microstructure with characteristic dendritic growth of celsian phase embedded in glass matrix.

### 3.5. Properties of GCs

The listing of the properties in Table 2 reveals the influence of firing temperature on shrinkage, density, and bending strength. In general, increase of both shrinkage and density values occurred over increasing temperature in the range of 850–950 °C. Shrinkage and density starts falling down in GCs 1 at 900 °C, which might be due to transformation of Mg-metasilicates. The incorporation of heavy elements, such as Y and Ba, causes significant increase of density. This phenomenon is more pronounced in the case of composition 3, which also features better crystallinity than compositions 1 and 2 that is a major factor for density increase. It should be noticed that the densities of celsian and Mg-metasilicates are of the same order of magnitude (3.2–3.3 g/cm$^3$ [2]).

Composition 2 demonstrated the highest mechanical strength values among the investigated compositions, although high mechanical strength was maintained in the compositions 1 and 3 at elevated temperatures, higher than 950 °C. The CTE value of the GCs 3 is higher than that of the GCs 1 and 2, likely due to formation of hexacelsian.

The stability of phase composition over increasing temperature, the relatively high values of bending strength and CTE of the GCs produced can be considered as favourable features for specific applications, such as insulators applied in electro-vacuum technology of joints with Ti (CTE 9–9.5 $\times$ 10$^{-6}$ [5]), or in the technology of solid oxide fuel cells (SOFC). Investigation of the electrical properties should be carried out to support the potential of the investigated compositions in other specific applications.

## 4. Conclusions

The influence of partial substitutions in cation and anion sublattice of Mg-metasilicate on the properties and the crystallization of the investigated glasses and GCs can be summarized as follows:

(a) The compositions 2 and 3 result in homogenous transparent glasses with good casting characteristics after melting at 1600 °C for 1 h, whereas longer melting is required for glasses of the composition 1.
(b) Mg-metasilicate phases (clino- and proto-enstatite) predominantly crystallized within a wide temperature range (GCs 1 and 2). There is evidence of Y substitution for Mg at 900–950 °C. The formation of hexacelsian that was crystallized together with clino-enstatite in the BaO-containing composition (GCs 3) was explained due to uptake of $Al_2O_3$ into the melt from alumina crucible.
(c) The stability of phases' assemblage within a wide temperature range together with the relatively high values of bending strength and CTE qualify the investigated GCs for further experimentation with regards to their use in specific technological applications, such as insulators for electro-vacuum techniques, joints with Ti, and in the technology of SOFC.

## Acknowledgement

Ashutosh Goel is indebted for the research fellowship grant from CICECO.

## References

[1] W. Höland, G.N. Beall, Glass-Ceramic Technology, The American Ceramic Society, Westerville, Ohio, 2002.
[2] W.E. Lee, A.H. Heuer, On the polymorphism of enstatite, J. Am. Ceram. Soc. 70 (1987) 349–360.
[3] C.M. Huang, D.H. Kuo, Y.J. Kim, W. Kriven, Phase stability of chemically derived enstatite ($MgSiO_3$) powders, J. Am. Ceram. Soc. 77 (1994) 2625–2631.
[4] G.H. Beall, Glass-ceramics: recent developments and applications, Ceram. Trans. 30 (1993) 241–266.
[5] V.L. Balkevich, Technical Ceramics, Stroiizdat, Moscow, 1984 (in Russian).
[6] W. Mielcarek, D. Nowak-Wozny, K. Prociow, Correlation between $MgSiO_3$ phases and mechanical durability of steatite ceramics, J. Eur. Ceam. Soc. 24 (2004) 3817–3821.
[7] D.U. Tulyaganov, S. Agathopoulos, V.V. Kharton, F.M.B. Marques, Glass-ceramics in the former Soviet Union: a review on industry-oriented developments, Ind. Ceram. 23 (2003) 101–115.
[8] E.A. Takher, T.I. Fedoseeva, V. Yu Kellerman, R. Ya Popilsky, High-strength steatite ceramics with broad range of the sintering stage, Glass Ceram. 2 (1974) 19–21.
[9] E.A. Takher, R. Ya Popilsky, V. Yu Kellerman, A.G. Sokolnikova, Dielectric steatite ceramics, Glass Ceram. 10 (1975) 19–21.
[10] G.N. Beall, Refractory glass-ceramic containing enstatite, US Patent 4 687 749, 18th August 1987.
[11] L.M. Echeverria, G.N. Beall, Enstatite ceramics: glass and gel routes, Ceram. Trans. 20 (1991) 235–244.
[12] G. Partridge, M.I. Budd, Toughened glass-ceramics, UK Patent GB 2172282, 17 September 1986.

[13] G. Partridge, M. Elyard, I. Budd, Glass-ceramics in substrate applications, in: M.H. Levis (Ed.), Glasses and Glass-Ceramics, Chapman and Hall, London, UK, 1989, pp. 226–271.
[14] M.I. Budd, Sintering and crystallization of a glass powder in the MgO–$Al_2O_3$–$SiO_2$–$ZrO_2$ system, J. Mater. Sci. 28 (1993) 1007–1014.
[15] M. Tribaudino, A transmission electron microscope investigation of the C2/c → $P2_1/c$ phase transition in clinopyroxenes along the diopside-enstatite ($CaMgSi_2O_6$-$Mg_2Si_2O_6$) join, Am. Miner. 85 (2000) 707–715.
[16] T. Gasparik, A thermodynamic model for the enstatite-diopside join, Am. Miner. 75 (1990) 1080–1091.
[17] Y. Ohashi, C.W. Burnham, L.W. Finger, The effect of Ca–Fe substitution on the clinopyroxene crystal structure, Am. Miner. 60 (1975) 423–434.
[18] V.I. Vereshchagin, E.P. Tzymbalyuk, B.P. Romanov, Correlation between crystalline structure and physico-technical properties of solid solutions in the system clinoenstatite-diopside, in: Nucleated Crystallization of Glasses, State Institute of Glass, Moscow, 1982 , pp. 95–100 (in Russian).
[19] D.U. Tulyaganov, S. Agathopoulos, J.M. Ventura, M.A. Karakassides, O. Fabrichnaya, J.M.F. Ferreira, Synthesis of glass-ceramics of CaO–MgO–$SiO_2$ system containing $B_2O_3$, $P_2O_5$ $Na_2O$ and $CaF_2$, J. Eur. Ceram. Soc. 26 (2006) 1463–1471.
[20] J. Fergus, Sealants for solid oxide fuel cells, J. Power Sources 147 (2005) 46–57.
[21] M. Oliveira, S. Agathopoulos, J.M.F. Ferreira, Reactions at the interface between $Al_2O_3$–$SiO_2$ ceramics with additives of alkaline earth oxides and liquid Al–Si alloy, J. Mater. Res. 17 (2002) 641–647.
[22] M. Oliveira, S. Agathopoulos, J. Lino, J.m.F. Ferreira, Interfacial reactions, thermodynamics and kinetics in doped aluminosilicate ceramics/liquid Al-alloy contacting systems, Mater. Sci. Forum 455–456 (2004) 639–643.